Hybrid Materials

DOI: 10.1002/anie.201302133

Well-Defined Nanofibers with Tunable Morphology from Spherical Colloidal Building Blocks**

Markus B. Bannwarth, Samuel W. Kazer, Sebastian Ulrich, Gunnar Glasser, Daniel Crespy, and Katharina Landfester**

Linear structures, such as actin filaments, muscle fibers, and hair, are ubiquitous in nature on various length scales and with different morphologies and periodicities. Mimicking these linear arrangements is attractive for many applications in fields ranging from energy conversion[1] and storage[2] to life sciences,[3] surface patterning,[4] and coatings.[5] The linear structures can promote, for instance, the directed transport of electrons or heat.[6] When linear nanostructures are modified further through the introduction of magnetic iron oxide moieties, they can be used for hyperthermia treatment,[7] high-performance lithium storage,[8] and as catalysts for the oxygen reduction reaction.[9] Desired properties often include nanometric dimensions, versatile labeling and functionalization, high stability, and magnetic loading with homogeneous distribution. In order to meet these criteria, organic–inorganic hybrid nanofibers are needed. Common approaches for the production of linear nanostructures include electrospinning,[10] magnetic-field-assisted electrospinning,[10c–d] self-assembly,[11] and template-assisted methods.[12] However, these approaches suffer drawbacks in terms of achieving combinations of the aforementioned desired properties. In contrast, the synthesis of spherical hybrid nanoparticles with multifunctionality is comparably easy and many variations have been reported.[13] A plethora of polymeric particles can be implemented for the formation of a two-dimensional film by sintering the particles together. Recently, one-dimensional (1D) as well as two-dimensional (2D) arrangements of microparticles were fabricated by making use of thermal annealing.[14] With the help of an elaborate templating matrix, more complex arrangements such as rings are possible.[15] However, a templating matrix can produce only small amounts of materials. A template-free fabrication of polymeric hybrid nanofibers in solution with defined architecture is therefore highly desirable.

Herein, we present a method for the facile and versatile linear fusion of magnetic polymer nanoparticles in an aqueous dispersion by the directed sintering of linear self-assembled magnetic nanoparticles. The strategy is thus suitable for the fabrication of hybrid polymer/inorganic nanofibers with tunable surface corrugation. The linear arrangement and the alignment of the particles are realized by their assembly upon an external magnetic field and a moderate flow of water. The environmental temperature is controlled to favor polymer chain diffusion so that the neighboring particles in contact with each other can fuse together.

The axial fusion of magnetic polymer colloids into nanofibers can be accomplished with a simple setup (Figure 1), which includes a thermostat and a pump for controlling the temperature and the flow of water, respectively. The functional particles are injected and transported to a permanent ring magnet (field strength 25–200 mT). The external magnetic field induces a magnetic dipole in each superparamagnetic nanoparticle. Due to attractive dipole–dipole interactions, the particles assemble in a linear fashion.[16] Particle fusion is achieved when the surrounding temperature of the aqueous environment is above the glass transition temperature (T_g) of the polymer. The formed fibers can be collected by increasing the flow speed and thereby displacing them from the magnet. The benefits of the process comprise the fast fabrication of nanofibers (fusion within milliseconds to seconds), simple equipment, and the aqueous medium. The topology of the nanofibers' surface can also be controlled by varying the degree of fusion of the spherical functional particles (Figure 2). Because the fusion is highly dependent on the temperature, the degree of fusion and therefore the surface topology is tuned by the temperature of the aqueous

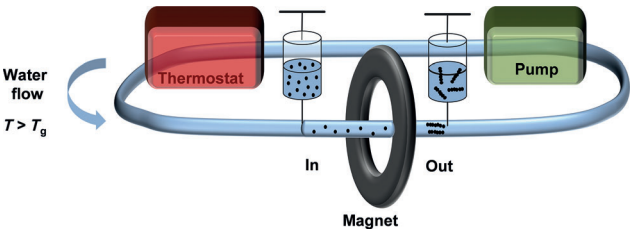

Figure 1. Experimental flow setup for the fabrication of nanofibers through magnetic self-assembly and linear fusion of magnetic polymer nanoparticles in aqueous dispersion.

[*] M. B. Bannwarth, S. W. Kazer, S. Ulrich, G. Glasser, Dr. D. Crespy, Prof. Dr. K. Landfester
Max Planck Institute for Polymer Research
Ackermannweg 10, 55128 Mainz (Germany)
E-mail: bannwart@mpip-mainz.mpg.de
landfester@mpip-mainz.mpg.de
M. B. Bannwarth
Graduate School Materials Science in Mainz
Staudinger Weg 9, 55128 Mainz (Germany)

[**] M.B.B. and S.W.K. gratefully acknowledge financial support by the Excellence Initiative (DFG/GSC 266) and the DAAD Rise program, respectively. We thank Prof. G. Jakob for VSM measurements, M. Steiert for XRD support, and Dr. I. Lieberwirth for helping with TEM imaging as well as Prof. H.-J. Butt, Dr. M. Kappl, and Dr. K. Koynov for fruitful discussions.

Supporting information for this article is available on the WWW under http://dx.doi.org/10.1002/anie.201302133.

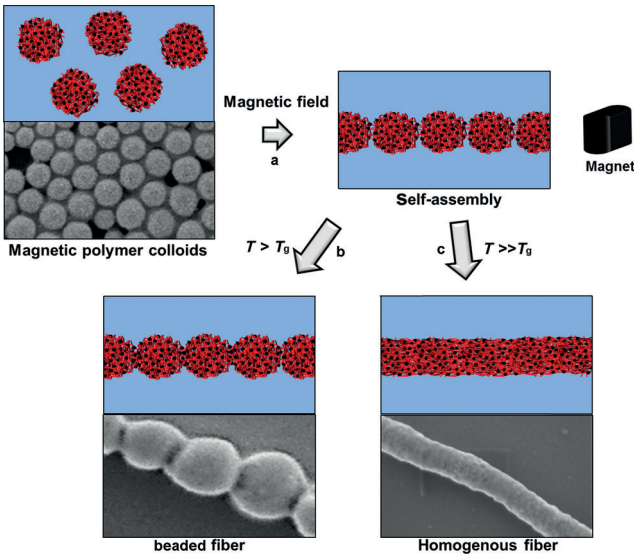

Figure 2. Magnetic self-assembly (a) and fusion (b,c) of magnetic polymer colloids in water. Increasing the temperature above the glass transition temperature (T_g) provides enough polymer chain flexibility and leads to a linear sintering process. Temperatures close to the T_g yield a low degree of fusion and a necklace-like morphology (b). For temperatures well above the T_g, a larger degree of fusion is observed and completely merged particles form a homogeneous fiber containing homogeneously distributed iron oxide nanoparticles (c).

medium. Architectures resembling necklaces are obtained by weakly fusing the particles, whereas almost uniform nanofibers are created for a higher degree of fusion. In the latter case, the identity of the single nanoparticles is lost, that is, the initial magnetic nanoparticles cannot be identified in the final nanofibers.

Superparamagnetic magnetite nanoparticles capped with oleate were used as magnetic moieties (see Figure S1 in the Supporting Information for details). Owing to their superparamagnetic properties, attractive forces between the magnetic particles are only present when an external magnetic field is applied. Thus, after the formation of fibers from the magnetic polymer colloids, no interaction between the fibers is observed when the external magnetic field is removed. As a consequence, a permanent linkage has to be generated when the particles are aligned. By introduction of a polymer matrix, the migration of polymer chains upon temperature increase leads to such a linkage. Therefore, polystyrene nanoparticles with encapsulated magnetite were employed as model polymer particles for fiber formation. For the synthesis, miniemulsion droplets with dispersed magnetic nanoparticles were used as seeds for the emulsion polymerization of styrene. Miniemulsion droplets were chosen since they can be modified readily through the integration of functional moieties (e.g. dyes, inorganic nanoparticles, functional monomers) into the droplets and therefore into the resulting nanoparticles.[13,17] To verify the feasibility of the linear sintering of self-assembled polymer particles, we first synthesized polystyrene nanoparticles with homogeneously distributed magnetite (PS-Mag-H). A high magnetite content was chosen (70 wt% according to thermogravimetric analysis (TGA) measurements) in order to achieve a large magnetic dipole in each particle under application of an external magnetic field and thus strong interparticle attraction.

Whereas the attraction between the particles can be tuned by the amount of magnetite inside the hybrid particles, the merging process is mainly controlled by the nature of the polymer for a defined continuous phase, for example, water in this case, and a given temperature. During the merging process, several events occur sequentially: 1) Deformation of the particles due to minimization of the interfacial energy between polymer and water leads to an increase in contact area between neighboring particles. The deformation is strongly dependent on the size of the particles.[18] 2) The diffusion of the polymer chains enables material exchange between the particles and merges the particles together. The molecular weight of the polymer chains and their polydispersity play a very important role for the kinetics of chain diffusion.[19]

The employed nanoparticles (PS-Mag-H) display a hydrodynamic diameter of (127 ± 8) nm as determined by dynamic light scattering (DLS). Owing to this relatively small diameter, the contribution of retarded elastic deformation to the sintering process is strong and thus supports colloid fusion.[18] Additionally, it offers the advantage that the resulting fibers are small in diameter and therefore have a large surface to volume ratio. To facilitate the facile merging of the hybrid nanoparticles, no crosslinker was used. The weight average molecular weight (M_w) of the polymer was determined to be 29400 g mol^{-1} with a polydispersity index (PDI) of 2.8. The relatively low molecular weight permits fast chain diffusion which is accelerated by the large PDI.[19] The T_g of the hybrid particles was measured to be 56 °C as determined by differential scanning calorimetry (DSC). The fact that the T_g of pure polystyrene (ca. 100 °C[20]) is significantly higher than that of the hybrid particles can be explained by the presence of oleic acid in the oleate-capped magnetic nanoparticles (Figure S3).

To obtain highly stable nanoparticles, the charged co-monomer styrene sulfonate was added during the polymerization to introduce a covalently bonded negative surface charge. The negatively charged surface (zeta potential of −51 mV) provides additional stabilization of the colloids by electrostatic repulsion between the particles which prevents their aggregation. Without the functional co-monomer, the polymer particles could still be merged together, but large nonlinear aggregates of particles were observed.

The length and structure of the formed nanofibers were investigated by scanning electron microscopy (SEM) and transmission electron microscopy (TEM; Figure 3). Under typical conditions (magnetic field of 200 mT, $T = 85$ °C, 10 s fusion time), the average length of the fibers was determined to be (6.4 ± 2.5) μm for PS-Mag-H. An average number of 55 ± 22 nanoparticles can be assigned to the fibers. The average length of the fibers can be controlled by varying the time of fusion (Figure S4). Following a fast increase in fiber length with the employed time of fusion, the length converges to a maximum. Additionally, we found that the amplitude of the magnetic field has an influence on the chain length. Application of a weaker field of 25 mT leads to the formation of shorter fibers (20–50% shorter). A flow velocity in the

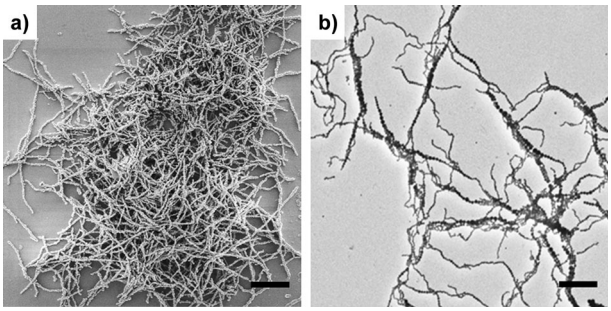

Figure 3. SEM (a) and TEM (b) images of nanofibers formed from polystyrene nanoparticles homogeneously loaded with iron oxide. Scale bar 2 μm.

range of 0.3–2 mm s^{-1} was found to be suitable. Once the fibers are formed, application of moderate sonication or vigorous stirring does not cause them to break. In a surfactant solution, the colloidal stability of the nanofibers can be maintained for several hours and it takes several days for the fibers to precipitate.

Since the environmental temperature is set above but close to the T_g of the polymer, the nanoparticle merging is slow and it is possible to investigate the kinetics of the merging process in detail (Figure 4). Therefore the average

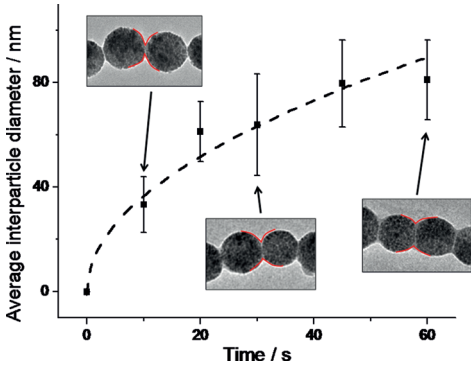

Figure 4. Temporal evolution of the interparticle diameter for the merging of PS-Mag-H particles.

interparticle diameter for PS-Mag-H was investigated as a function of the time of merging. According to Frenkel's theory of sintering, the interparticle radius (or diameter) between two particles is proportional to the square root of the sintering time.[21] Because the merging kinetics of the PS-Mag-H particles could be described by this theory (Figure 4), the interparticle diameter can be controlled and predicted.

Detailed investigations of the internal fiber morphology and distribution of magnetic nanoparticles inside the polymer matrix were carried out by TEM imaging (Figure 5). Figure 5A shows the TEM image of a beaded nanofiber with weakly merged particles. The contact area between neighboring particles displays mainly polystyrene and only very little amount of magnetite. The particle is slightly elongated along the fiber axis (aspect ratio of 1.07:1.00). For completely merged particles (Figure 5B), the inorganic nanoparticles are

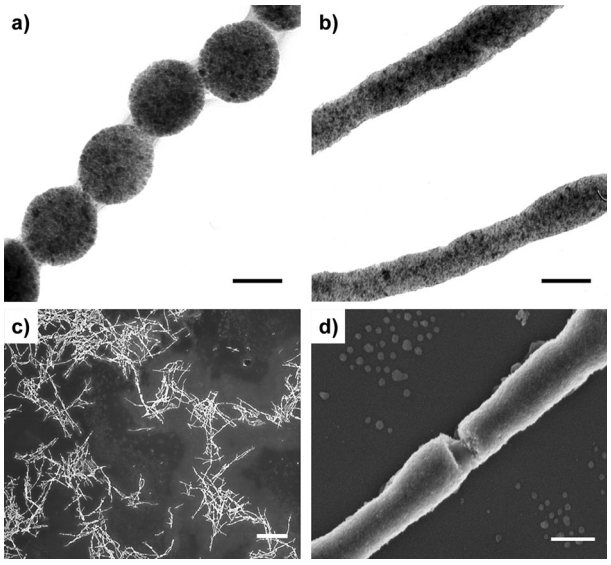

Figure 5. TEM images of linear merged polystyrene nanoparticles loaded with iron oxide. Weak merging of PS-Mag-H particles leads to beaded structures (a), higher degree of merging yields relatively smooth nanofibers in which single particles cannot be identified (b). SEM images of calcined, strongly fused PS-Mag-H nanofibers: Overview (c) and close-up (d). Scale bars: 100 nm (a,b,d); 5 μm (c).

homogeneously distributed along the polymer fiber. These observations indicate that the mechanism of particle merging is composed of different steps depending on the temperature: 1) For temperatures close to the T_g, elastic deformation of the particles leads to a weak overlap of the particles and a slight particle anisotropy. Interparticle diffusion of single polymeric chains and entanglements leads to the linkage of neighboring particles. The iron oxide remains mainly static. 2) At higher fusion temperatures, higher flexibility and stronger deformation of the particles are observed. The large deformation increases the contact area between neighboring particles, which leads to enhanced exchange of material between the particles. Additionally, the polymer chain diffusion is increased and the iron oxide nanoparticles can be distributed together with the polymer chains. As a consequence, nanofibers with homogeneously distributed iron oxide nanoparticles are obtained. With a further increase in temperature, a slight increase in the average diameter of the fibers can be observed. This can be attributed to the reduction of interfacial energy between the hybrid material and water owing to a decrease the aspect ratio of the nanofibers.

The hybrid fibers can be further calcined to obtain inorganic nanofibers and nanorods (Figure 5c,d). When the completely merged particles PS-Mag-H are calcined, the homogeneously distributed iron oxide nanoparticles prevent the wires from cracking and iron oxide nanostructures with high aspect ratio (ca. 22) can be obtained (Figure S5). However, at certain points in the fibers, the calcination leads to breaking points that yield magnetic inorganic nanorods. A three-dimensional network of iron oxide can be obtained. Owing to their high aspect ratios, their thin diameters, and their porous structures, these iron oxide nanorods are promising candidates as building blocks for

the catalysis of oxygen reduction reaction[9] or for high-performance lithium storage.[8]

Going one step further, we synthesized nanoparticles with a more complex Janus morphology (PS-Mag-J) and applied the aforementioned process. The variation of colloidal morphology induced an alignment of the particles in a zigzag fashion upon application of an external magnetic field.[22] The conditions for merging the Janus particles are more challenging than those for PS-Mag-H. The reasons are the lower iron oxide loading (34 wt%), which leads to weaker interaction of the particles in the magnetic field, the larger particles size (237 ± 27 nm), which slows down the particle deformation, and the higher molecular weight of the polymer ($M_w = 158000\ g\,mol^{-1}$, PDI = 5.0), which enhances the viscosity of the heated particles. Nevertheless, the particles can be successfully merged together (Figure 6). The obtained zigzag architectures have an average length of (3.0 ± 1.1) μm with an average number of particles per fiber of 13 ± 4. The zigzag fibers are significantly shorter and consist of fewer particles than PS-Mag-H because of the lower magnetic attraction force and the difficult zigzag arrangement. This arrangement not only requires diffusion of the particles into linear structures, but additionally rotation into the right orientation. The particles merge together in a two-dimensional plane and therefore have only one orientational possibility in this plane. For the Janus nanoparticles, a weak (c) and a stronger (d) fusion can be observed as for PS-Mag-H. However, in the case of stronger fusion, the Janus particles do not form smooth cylindrical fibers. This difference in comparison to PS-Mag-H can be explained by the significantly higher molecular weight of the polymer in the Janus nanoparticles and the resulting higher viscosity of the polymer chains,[23] which slows down the diffusion significantly.

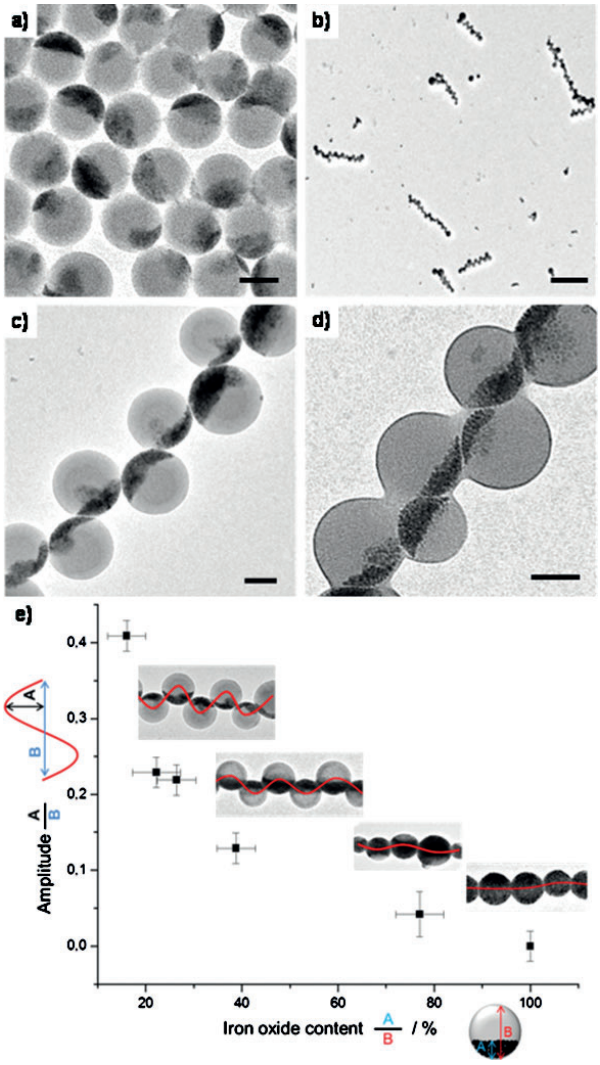

Figure 6. TEM images of PS-Mag-J nanoparticles (a) and zigzag fibers (b,c,d). Weakly fused zigzag fiber (c) and stronger fused fiber (d). Scale bars: 200 nm (a,c,d); 2 μm (b). Control of corrugation amplitude by variation of iron oxide content (e).

Furthermore, the zigzag corrugation can be controlled by the ratio of iron oxide to polystyrene within the Janus particles (Figure 6e). Indeed, decreasing the iron oxide content results in more pronounced corrugation in the zigzag fibers.

In conclusion, we have demonstrated a novel method for the preparation of hybrid and inorganic fibers and nanorods in aqueous environments. Spherical magnetic building blocks of hybrid nanoparticles are assembled in an aqueous flow and an external magnetic field without any templating agent. The fast fusion speed (0.5–50 s), the facile synthetic procedure, and the aqueous fusion medium are important advantages of this novel process. The morphology of the obtained fibers, ranging from necklace-like to smooth cylindrical structures with tuneable corrugation, can be controlled by process parameters such as time of fusion and temperature, and by the morphology of the magnetic nanoparticles. The assembly of Janus nanoparticles yields zigzag structures. The complexity of the 0D initial structure is therefore used for inducing a complexity into the obtained 1D structure. It is expected that novel supraparticular assemblies with high stability will be created by using spherical building blocks of different sizes and with more complex colloidal structures.

Received: March 13, 2013
Published online: July 23, 2013

Keywords: hybrid materials · nanofibers · nanorods · self-assembly · superparamagnetism

[1] a) P. Reineck, G. P. Lee, D. Brick, M. Karg, P. Mulvaney, U. Bach, *Adv. Mater.* **2012**, *24*, 4750–4755; b) D. L. Long, E. Burkholder, L. Cronin, *Chem. Soc. Rev.* **2007**, *36*, 105–121.
[2] a) D. H. Wang, R. Kou, D. Choi, Z. G. Yang, Z. M. Nie, J. Li, L. V. Saraf, D. H. Hu, J. G. Zhang, G. L. Graff, J. Liu, M. A. Pope, I. A. Aksay, *ACS Nano* **2010**, *4*, 1587–1595; b) S. Cavaliere, S. Subianto, I. Savych, D. J. Jones, J. Roziere, *Energy Environ. Sci.* **2011**, *4*, 4761–4785.
[3] a) Y. Z. Long, M. Yu, B. Sun, C. Z. Gu, Z. Y. Fan, *Chem. Soc. Rev.* **2012**, *41*, 4560–4580; b) G. F. Zheng, F. Patolsky, Y. Cui, W. U. Wang, C. M. Lieber, *Nat. Biotechnol.* **2005**, *23*, 1294–1301.
[4] J. Y. Cheng, C. T. Rettner, D. P. Sanders, H. C. Kim, W. D. Hinsberg, *Adv. Mater.* **2008**, *20*, 3155–3158.
[5] S. Srinivasan, V. K. Praveen, R. Philip, A. Ajayaghosh, *Angew. Chem.* **2008**, *120*, 5834–5838; *Angew. Chem. Int. Ed.* **2008**, *47*, 5750–5754.

[6] S. Shen, A. Henry, J. Tong, R. T. Zheng, G. Chen, *Nat. Nanotechnol.* **2010**, *5*, 251 – 255.
[7] C. Huang, S. J. Soenen, J. Rejman, J. Trekker, L. Chengxun, L. Lagae, W. Ceelen, C. Wilhelm, J. Demeester, S. C. De Smedt, *Adv. Funct. Mater.* **2012**, *22*, 2479 – 2486.
[8] S. Yang, Y. Sun, L. Chen, Y. Hernandez, X. Feng, K. Müllen, *Sci. Rep.* **2012**, 2, 427.
[9] Z. H. Wen, S. Q. Ci, F. Zhang, X. L. Feng, S. M. Cui, S. Mao, S. L. Luo, Z. He, J. H. Chen, *Adv. Mater.* **2012**, *24*, 1399 – 1404.
[10] a) A. Greiner, J. H. Wendorff, *Angew. Chem.* **2007**, *119*, 5770 – 5805; *Angew. Chem. Int. Ed.* **2007**, *46*, 5670 – 5703; b) D. Crespy, K. Friedemann, A. M. Popa, *Macromol. Rapid Commun.* **2012**, *33*, 1978 – 1995.
[11] a) Z. Junfeng, M. Lingjie, F. Xinliang, Z. Xiaoke, L. Qinghua, *Angew. Chem.* **2007**, *119*, 5770 – 5805; *Angew. Chem. Int. Ed.* **2010**, *49*, 8476 – 8479; b) A. J. Amali, P. Saravanan, R. K. Rana, *Angew. Chem.* **2011**, *123*, 1354 – 1357; *Angew. Chem. Int. Ed.* **2011**, *50*, 1318 – 1321; c) K. S. Khalil, A. Sagastegui, Y. Li, M. A. Tahir, J. E. S. Socolar, B. J. Wiley, B. B. Yellen, *Nat. Commun.* **2012**, *3*, 794; d) H. Singh, P. E. Laibinis, T. A. Hatton, *Langmuir* **2005**, *21*, 11500 – 11509; e) R. Sheparovych, Y. Sahoo, M. Motornov, S. M. Wang, H. Luo, P. N. Prasad, I. Sokolov, S. Minko, *Chem. Mater.* **2006**, *18*, 591 – 593; f) K. Liu, Z. H. Nie, N. N. Zhao, W. Li, M. Rubinstein, E. Kumacheva, *Science* **2010**, *329*, 197 – 200.
[12] a) L. Shi, C. J. Pei, Y. M. Xu, Q. Li, *J. Am. Chem. Soc.* **2011**, *133*, 10328 – 10331; b) P. N. Martinho, T. Lemma, B. Gildea, G. Picardi, H. Muller-Bunz, R. J. Forster, T. E. Keyes, G. Redmond, G. G. Morgan, *Angew. Chem.* **2012**, *124*, 12161 – 12165; *Angew. Chem. Int. Ed.* **2012**, *51*, 11995 – 11999.
[13] K. Landfester, *Angew. Chem.* **2009**, *121*, 4556 – 4576; *Angew. Chem. Int. Ed.* **2009**, *48*, 4488 – 4507.
[14] H. R. Vutukuri, J. Stiefelhagen, T. Vissers, A. Imhof, A. van Blaaderen, *Adv. Mater.* **2012**, *24*, 412-416.
[15] Y. N. Xia, Y. D. Yin, Y. Lu, J. McLellan, *Adv. Funct. Mater.* **2003**, *13*, 907 – 918.
[16] a) Y. Lin, A. Boker, J. B. He, K. Sill, H. Q. Xiang, C. Abetz, X. F. Li, J. Wang, T. Emrick, S. Long, Q. Wang, A. Balazs, T. P. Russell, *Nature* **2005**, *434*, 55 – 59; b) C. B. Mao, D. J. Solis, B. D. Reiss, S. T. Kottmann, R. Y. Sweeney, A. Hayhurst, G. Georgiou, B. Iverson, A. M. Belcher, *Science* **2004**, *303*, 213 – 217; c) S. Y. Park, H. Handa, A. Sandhu, *Nano Lett.* **2010**, *10*, 446 – 451; d) R. M. Erb, H. S. Son, B. Samanta, V. M. Rotello, B. B. Yellen, *Nature* **2009**, *457*, 999 – 1002.
[17] K. Landfester, *Annu. Rev. Mater. Res.* **2006**, *36*, 231 – 279.
[18] S. Mazur, R. Beckerbauer, J. Buckholz, *Langmuir* **1997**, *13*, 4287 – 4294.
[19] M. Soleimani, S. Khan, D. Mendenhall, W. Lau, M. A. Winnik, *Polymer* **2012**, *53*, 2652 – 2663.
[20] H. Gausepohl, *Kunststoff-Handbuch*, Hanser Verlag, München, **1996**.
[21] R. E. Dillon, L. A. Matheson, E. B. Bradford, *J. Colloid Sci.* **1951**, *6*, 108 – 117.
[22] a) D. Zerrouki, J. Baudry, D. Pine, P. Chaikin, J. Bibette, *Nature* **2008**, *455*, 380 – 382; b) J. Yan, M. Bloom, S. C. Bae, E. Luijten, S. Granick, *Nature* **2012**, *491*, 578 – 581.
[23] W. M. Kulicke, R. Kniewske, *Rheol. Acta* **1984**, *23*, 75 – 83.

